Geophysical Research Letters

RESEARCH LETTER
10.1029/2019GL082756

Pacing of Red Sea Deep Water Renewal During the Last Centuries

Thomas Felis[1] and **Manfred Mudelsee**[2,3]

[1]MARUM - Center for Marine Environmental Sciences, University of Bremen, Bremen, Germany, [2]Climate Risk Analysis, Bad Gandersheim, Germany, [3]Alfred Wegener Institute Helmholtz Centre for Polar and Marine Research, Bremerhaven, Germany

Key Points:
- Observed frequent late twentieth century Red Sea deep water renewals were probably unusual in the context of the preceding ~100 years
- Coral proxy record suggests absence of major deep water formation events until the 1883 Krakatau volcanic eruption
- More frequent major Red Sea deep water formation events are detected during the early nineteenth century and late Little Ice Age

Supporting Information:
- Supporting Information S1

Correspondence to:
T. Felis,
tfelis@marum.de

Citation:
Felis, T., & Mudelsee, M. (2019). Pacing of Red Sea deep water renewal during the last centuries. *Geophysical Research Letters*, *46*, 4413–4420. https://doi.org/10.1029/2019GL082756

Received 8 MAR 2019
Accepted 2 APR 2019
Accepted article online 5 APR 2019
Published online 23 APR 2019

Abstract The Red Sea is a deep marine basin often considered as small-scale version of the global ocean. Hydrographic observations and ocean-atmosphere modeling indicate Red Sea deep water was episodically renewed by wintertime open-ocean deep convections during 1982–2001, suggesting a renewal time on the order of a decade. However, the long-term pacing of Red Sea deep water renewals is largely uncertain. We use an annually resolved coral oxygen isotope record of winter surface water conditions to show that the late twentieth century deep water renewals were probably unusual in the context of the preceding ~100 years. More frequent major events are detected during the late Little Ice Age, particularly during the early nineteenth century characterized by large tropical volcanic eruptions. We conclude that Red Sea deep water renewal time is on the order of a decade up to a century, depending on the mean climatic conditions and large-scale interannual climate forcing.

Plain Language Summary The Red Sea is a deep marine basin often considered as small-scale version of the global ocean. Hydrographic observations and ocean-atmosphere modeling indicate Red Sea deep water was episodically renewed by wintertime open-ocean deep convections in the northern Red Sea during 1982–2001, suggesting a deep water renewal time on the order of a decade. However, the long-term pacing of Red Sea deep water renewals is largely uncertain, due to lack of hydrographic observations. By using an annually resolved coral oxygen isotope record of winter surface water conditions in the northern Red Sea we show that the late twentieth century deep water renewals were probably unusual in the context of the preceding ~100 years. Our results suggest an absence of major deep water formation events until the 1883 Krakatau volcanic eruption. More frequent major events are detected during the late Little Ice Age, particularly during the early nineteenth century characterized by large tropical volcanic eruptions. From our long-term perspective we conclude that Red Sea deep water renewal time is on the order of a decade up to a century, depending on the mean climatic conditions and large-scale interannual climate forcing, which should be considered in management strategies of its unique ecosystems.

1. Introduction

The Red Sea represents a unique marine environment that has been used to derive fundamental constraints on global sea level variations during the last five glacial-interglacial cycles (Rohling et al., 2009) and the isotopic composition and origin of geothermal brines (Craig, 1966). Despite its relatively small size, important similarities to the world ocean have been noted. These include processes of convective and subductive water mass formation driving thermohaline meridional overturning circulation, and atmosphere-ocean interactions leading to water mass formation events (Eshel & Naik, 1997). The Red Sea is connected to the Indian Ocean in the south by the shallow (137-m deep) Strait of Bab el Mandeb. It is occupied by a nearly homogeneous, warm (~21.5 °C) and highly saline (~40.5) deep water mass extending from intermediate depths (~137 to 300 m) down to over 2,000 m (Yao & Hoteit, 2018). Due to very sparse hydrographic observations, the processes and pacing of Red Sea deep water renewals over longer timescales have been a topic of debate for almost 50 years. Previous work suggested that Red Sea deep water is mainly ventilated, continuously or intermittently, in the northern Red Sea by dense outflows from the Gulf of Suez and the Gulf of Aqaba, with a resulting sluggish renewal time on the order of 36 to 90 years (Cember, 1988; Eshel et al., 1994; Woelk & Quadfasel, 1996). A recent study (Yao & Hoteit, 2018), however, has used repeated hydrographic observations and simulations of an ocean general circulation model with realistic atmospheric forcing to show that large portions of the Red Sea deep water were episodically renewed during 1982–2001 by

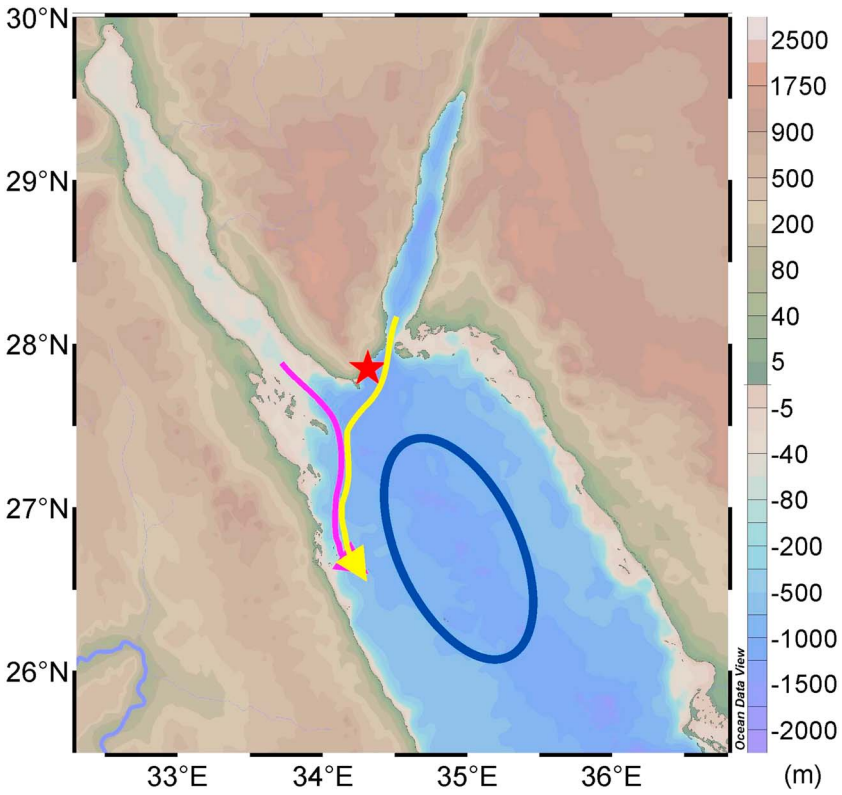

Figure 1. Map of the northern Red Sea. The processes of deep water formation in the northern Red Sea from three different sources are schematically indicated (Yao & Hoteit, 2018). Open-ocean deep convection in the interior of the basin (blue oval) and dense outflows from the Gulfs of Suez (pink arrow) and Aqaba (yellow arrow). The coral site at Ras Umm Sidd (Felis et al., 2000, red star) near the southern tip of the Sinai Peninsula is directly exposed to open northern Red Sea waters. Map created with Ocean Data View (Schlitzer, 2018).

new dense waters mainly formed by open-ocean deep convections in the northern Red Sea. These rapid Red Sea deep water renewals occurred in anomalously cold winters either following large tropical volcanic eruptions or characterized by a strong positive phase of the North Atlantic Oscillation (NAO, Yao & Hoteit, 2018). The results suggest a much shorter renewal time for Red Sea deep water on the order of a decade (Yao & Hoteit, 2018), but direct evidence for deep water formation events throughout the last century and beyond is lacking. Importantly, the northern Red Sea probably *is the only place on Earth in which deep water forms where corals grow* (Eshel et al., 2000), and the oxygen isotope signal ($\delta^{18}O$) in coral skeletons serves as proxy for surface water density and deep water formation (Eshel et al., 2000).

2. Materials and Methods

An annually resolved proxy time series of winter conditions in northern Red Sea surface waters was obtained from a bimonthly resolved $\delta^{18}O$ record (Felis et al., 2000) of a shallow-water coral growing near the southern tip of the Sinai Peninsula (Figure 1). The time series was derived from the annual winter maxima of the seasonal cycles of $\delta^{18}O$ (Felis, 2001; Felis et al., 2000, supporting information Text S1), representing conditions during late boreal winter when Red Sea deep water renewals occur (Yao & Hoteit, 2018, January through March). The $\delta^{18}O$ signal in corals reflects a combination of both the temperature and the $\delta^{18}O$ composition of ambient seawater at the time of skeleton precipitation. Seawater $\delta^{18}O$, in general, closely reflects salinity, which in the arid northern Red Sea is controlled primarily by surface evaporation (Eshel et al., 2000; Felis et al., 2018, 2000). Essentially, we consider coral $\delta^{18}O$ as an indicator of surface water density and hence a potential quantitative proxy of deep water formation (Eshel et al., 2000). The winter coral $\delta^{18}O$ time series was calibrated with modeled changes in the total volume of the annual contributions from open-ocean deep convection and combined outflows from the Gulfs of Suez and Aqaba to wintertime deep water formation in

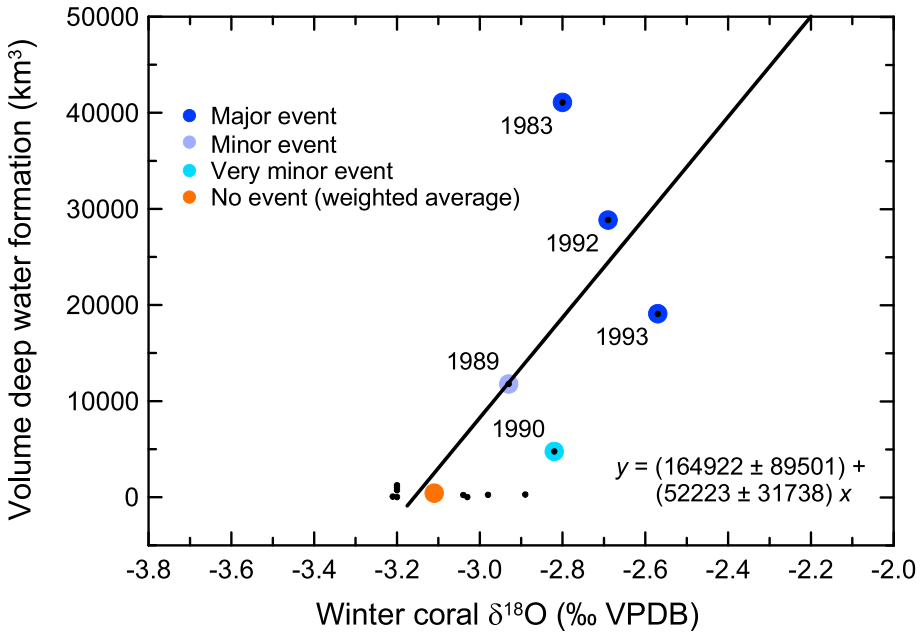

Figure 2. Regression of deep water formation volume on northern Red Sea coral $\delta^{18}O$. Ordinary least squares regression with bias correction (OLSBC, Text S1) on winter coral $\delta^{18}O$ was applied to the modeled changes in the total volume of annual contributions from open-ocean deep convection and combined outflows from the Gulfs of Suez and Aqaba to wintertime deep water formation in the northern Red Sea (Yao & Hoteit, 2018). Data points ($n = 6$) consist of five event years and the weighted average of the nine nonevent years during the period of overlap (1982–1995). From this we define major deep water formation events as having a total volume of >20,000 km^3 or coral $\delta^{18}O > -2.78‰$.

the northern Red Sea, as derived from simulations of an ocean general circulation model with realistic atmospheric forcing (Yao & Hoteit, 2018, Text S1). An ordinary least squares regression with bias correction (Mudelsee, 2014, OLSBC) reveals a significant relationship between total volume of deep water formation in a given winter and corresponding winter coral $\delta^{18}O$ (~52,000 ± 32,000 km^3 / per mil, Figure 2). Based on the regression, we define a major deep water formation event as having a total volume of >20,000 km^3. Under the assumption that the derived calibration equation holds over the time interval covered by the coral record, we provide estimates of significance for the occurrence of major Red Sea deep water renewals back into the late Little Ice Age (LIA) until the year 1751.

3. Red Sea Deep Water Formation During the Last Centuries

Surprisingly, the winter coral $\delta^{18}O$ time series shows no clear indications for major Red Sea deep water renewals during a relatively long ~100-year time interval prior to the 1982–1995 calibration period (Figure 3 and Table 1). The first major deep water formation event back in time is indicated for the year 1883 (±1), for which it is extremely likely (99.9%) that the documented winter coral $\delta^{18}O$ event exceeds the 20,000 km^3 threshold of the total volume of deep water formation. Comparable events are indicated for the years 1874 (±1) and 1863 (±1). Interestingly, more frequent major Red Sea deep water formation events compared to the following 150 years are indicated for the late LIA (~1750–1850), particularly for the first half of the nineteenth century. Prominent clusters of major deep water renewals are indicated for the middle to late 1830s and the middle 1750s to early 1760s. In addition, prominent major events occur in the years 1826 (±1), 1817 (±1), and 1791 (±1).

4. Red Sea Deep Water Formation and Large Volcanic Eruptions

We note a coincidence of reconstructed major Red Sea deep water renewals with large volcanic eruptions over the past 250 years (Figures 3 and 4 and Table 1). Evidence from observations and modeling during 1982–2001 indicates that significant deep water formation events occurred in the Red Sea in winters following years with large tropical volcanic eruptions (Yao & Hoteit, 2018), for example, in the late winter of 1992

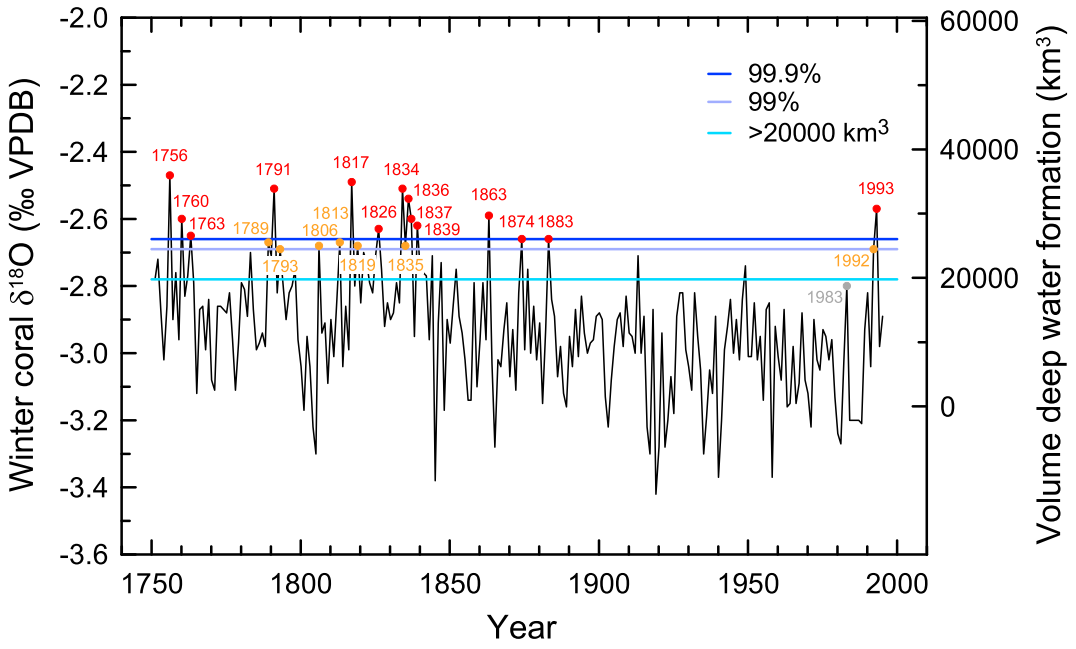

Figure 3. Annual coral proxy record of major Red Sea deep water renewals. Northern Red Sea winter coral $\delta^{18}O$ record (Felis, 2001; Felis et al., 2000) and inferred major Red Sea deep water formation events, as derived from calibration with modeled changes in total volume of deep water formation (Yao & Hoteit, 2018, Figure 2). Years for which it is extremely likely (99.9%, red) and very likely (99%, orange) that the documented winter coral $\delta^{18}O$ event exceeds the 20,000 km^3 threshold are indicated.

Table 1
Reconstructed Major Red Sea Deep Water Renewals and Potential Relationship to Large Volcanic Eruptions

Deep water formation year		Volcanic eruption year	Volcano	Latitude	VEI	VSSI eVolv2k_v2 (Tg)	GTSSAI IVI2_v2 (Tg)
1993							
1992		**1991**	**Pinatubo (Philippines)**	**15.13°N**	**6**	-	**30.1**
1883	±1	**1883**	**Krakatau (Indonesia)**	**6.10°S**	**6**	**9.3**	**21.9**
1874	±1	1873	Grímsvötn (Iceland)	64.42°N	4	1.2	-
1863	±1	**1861–62**	**Makian (Indonesia)**	**0.32°N**	**4**	**4.5**	**4.2**
1839	±1						
1837	±1						
1836	±1	**1835**	**Cosigüina (Nicaragua)**	**12.98°N**	**5**	**9.5**	**40.2**
1835	±1						
1834	±1						
1826	±1						
1819	±1						
1817	±1	**1815**	**Tambora (Indonesia)**	**8.25°S**	**7**	**28.1**	**109.7**
1813	±1						
1806	±1						
1793	±1						
1791	±1						
1789	±1						
1763	±2	**1761/62**	**unidentified**	**tropics**	-	**4.8**	**12.9**
1760	±2						
1756	±2	1755	Katla (Iceland)	63.63°N	5	1.2	8.0

Note. Reconstructed major deep water formation years when winter coral $\delta^{18}O$ extremely likely (99.9%, bold) or very likely (99%) exceeded the 20,000 km^3 total volume threshold (see Figures 2, 3, and Text S1 for details). Proposed matches to large tropical (bold) and large extratropical (normal type) volcanic eruptions. Eruption years and Volcanic Explosivity Index (VEI) from volcanoes of the world database (Global Volcanism Program, 2013). Attribution of volcanic stratospheric sulfur injection (Toohey & Sigl, 2017, VSSI) and global total stratospheric sulfate aerosol injection (GTSSAI, Gao et al., 2008) from ice core signals to specific eruptions according to Robock (2015) and Toohey and Sigl (2017), except for 1861 and 1755 in IVI2_v2. A tropical eruption of unknown origin is suggested by eVolv2k_v2 for 1762 (Toohey & Sigl, 2017) and IVI2_v2 for 1761 (Gao et al., 2008).

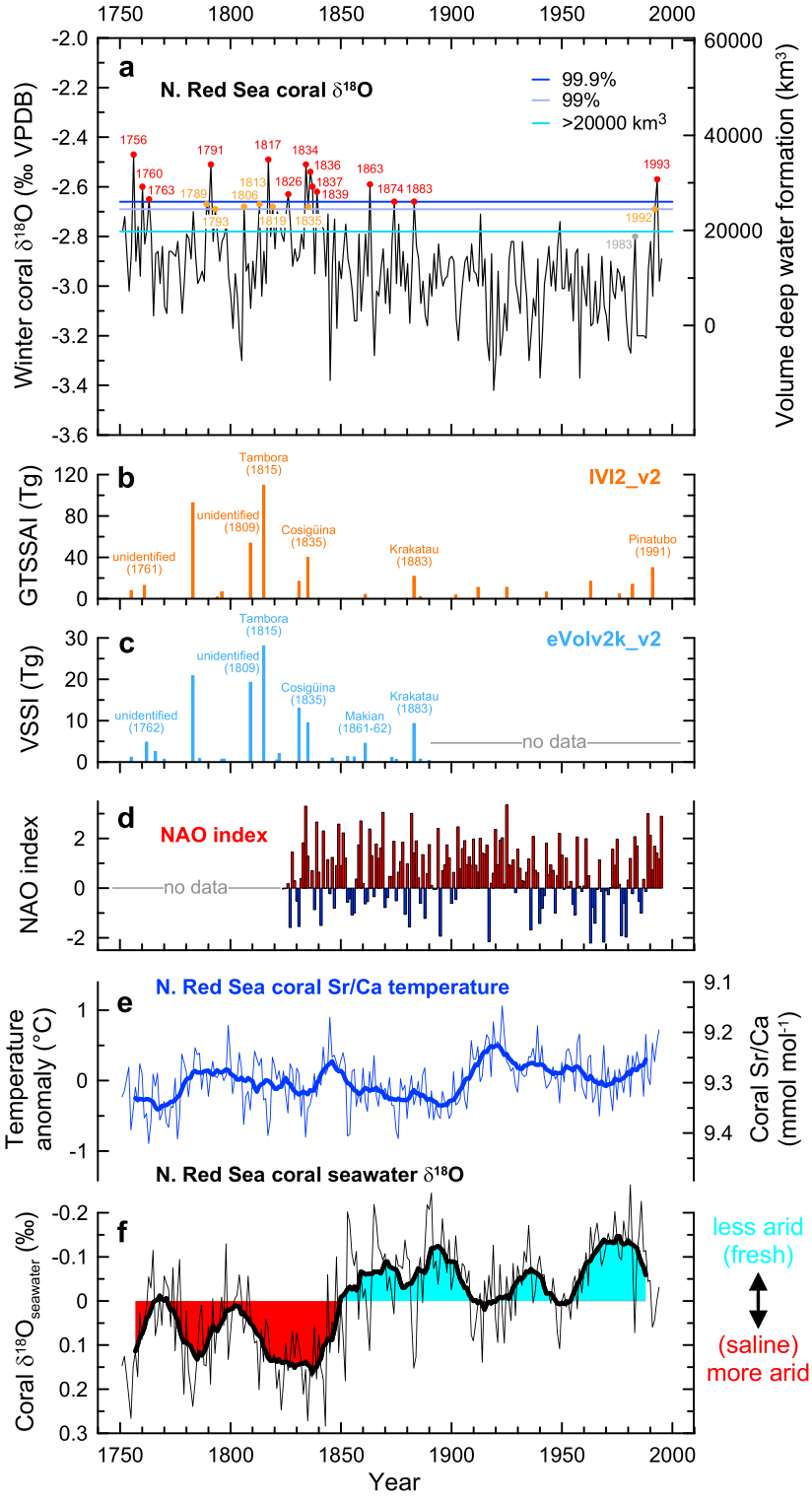

Figure 4. Annual coral proxy record of major Red Sea deep water renewals. (a) Northern Red Sea winter coral $\delta^{18}O$ record (Felis, 2001; Felis et al., 2000) and inferred major Red Sea deep water formation events. Years for which it is extremely likely (99.9%, red) and very likely (99%, orange) that the documented winter coral $\delta^{18}O$ event exceeds the 20,000 km^3 threshold are indicated. (b) Global total stratospheric sulfate aerosol injection (GTSSAI) from IVI2_v2 data set (Gao et al., 2008). (c) Volcanic stratospheric sulfur injection (VSSI) from eVolv2k_v2 data set (Toohey & Sigl, 2017). Attribution of ice core signals to specific tropical volcanic eruptions according to Robock (2015) and Toohey and Sigl (2017). (d) North Atlantic Oscillation (NAO) index (Jones et al., 1997; Osborn, 2011, December-January-February; 1951–1980 reference period). (e) Northern Red Sea annual average Sr/Ca temperature proxy record and annual seawater $\delta^{18}O$ reconstruction (coral $\delta^{18}O_{seawater}$) (f) derived from the same coral (Felis et al., 2018). Bold lines: 13-year running averages.

(January through March) following the 1991 Pinatubo eruption (Philippines) in the preceding year. Our reconstruction shows a number of five potential *matches* to large tropical eruptions prior to the 1982–1995 calibration period. This results when considering (1) the chronological error of the winter coral $\delta^{18}O$ time series of ±1 years for the interval 1924–1783 to ±2 years (1782–1751) and (2) that the coral proxy record represents conditions during late winter when Red Sea deep water renewals occur (Yao & Hoteit, 2018, January through March), that means, a relevant eruption needs to have occurred in the preceding year. Following these criteria, an extremely likely (99.9%) deep water formation event in the year 1883 (±1) potentially coincides with the 1883 eruption of Krakatau (Indonesia), one in 1863 (±1) with the 1861–1862 Makian eruption (Indonesia), one in 1836 (±1) with the 1835 Cosigüina eruption (Nicaragua), one in 1817 (±1) with the famous 1815 Tambora eruption (Indonesia) that caused the 1816 *year without a summer* in Europe (Luterbacher & Pfister, 2015; Robock, 2015), and one in 1763 (±2) with an unidentified eruption of probably tropical origin in 1761 or 1762. We note the absence of an event that could be associated with the unidentified major tropical eruption in 1809. In the light of recent evidence for a larger role of extratropical volcanic eruptions in Northern Hemisphere surface cooling (Toohey et al., 2019), we note two potential *matches* to large extratropical eruptions. Two extremely likely (99.9%) deep water formation events in 1874 (±1) and 1756 (±2) potentially coincide with the eruptions of Grímsvötn (1873) and Katla (1755) on Iceland (Table 1). However, the chronological error of the coral time series prior to 1925 impedes a more detailed analysis of the large-scale atmospheric circulation pattern and volcanic eruption-climate connection during the suggested event years.

5. Red Sea Deep Water Formation and Arctic Oscillation/NAO

Instrumental observations show that large tropical volcanic eruptions can change the large-scale atmospheric circulation toward a more positive phase of the Arctic Oscillation (AO)/NAO, resulting in Middle Eastern cooling in the first winter after the eruption (Robock & Mao, 1992; Yao & Hoteit, 2018; Zambri & Robock, 2016). In addition to the cooling, the regional atmospheric circulation during the positive AO/NAO phase enhances surface evaporation in the northern Red Sea (Eshel et al., 2000; Felis et al., 2000; Rimbu et al., 2001). The combined effect of cooling and evaporation increases surface water density favoring Red Sea deep water formation and is amplified in the coral $\delta^{18}O$ proxy signal (Eshel et al., 2000; Felis et al., 2018, 2000). Of course, a strong positive AO/NAO phase also occurs in winters without preceding large tropical volcanic eruptions, for example, in the late winter of 1989 characterized by a NAO index of +3.00 (December-January-February, DJF; Jones et al., 1997; Osborn, 2011) when Red Sea deep water formation occurred (Yao & Hoteit, 2018, Figure 2). Potential examples for such years in our reconstruction of major Red Sea deep water renewals are two extremely likely (99.9%) deep water formation events in 1839 (±1) and 1834 (±1) that coincide with strong positive NAO winters in 1839 (+2.66, DJF; Jones et al., 1997; Osborn, 2011) and 1834 (+3.30, DJF; Jones et al., 1997; Osborn, 2011, Figures 3 and 4), respectively. Considering the chronological error of the winter coral $\delta^{18}O$ time series, the two extremely likely (99.9%) deep water formation events in 1883 (±1) and 1863 (±1) attributed to the 1883 Krakatau and the 1861–1962 Makian eruption potentially coincide with the strong positive NAO winters in 1882 (+3.01, DJF) and 1863 (+2.25, DJFM; Jones et al., 1997; Osborn, 2011), respectively. Thus, the presented coral evidence suggests some linkage between Red Sea deep water renewals and AO/NAO forcing during the nineteenth century, in addition to the atmospheric forcing by large tropical volcanic eruptions.

6. Red Sea Deep Water Formation and Interannual/Mean Climate

An exception is the observed major Red Sea deep water formation event during the calibration period in the late winter of 1983 (Figure 2) following the large tropical 1982 El Chichón eruption (Mexico, Woelk & Quadfasel, 1996; Yao & Hoteit, 2018). Interestingly, although recorded, this is not represented as significant major event in the winter coral $\delta^{18}O$ time series (Figure 3). The limits of the reconstruction based on a single proxy record (finite spatial resolution, coral biomineralization and physiology issues) may be overcome by means of replicated coral records from multiple northern Red Sea sites in future studies. Furthermore, we cannot completely exclude the occurrence of major Red Sea deep water renewals during the ~100-year-long time interval (1884–1981) prior to the calibration period, where two events (in 1949 and 1913) exceed the 20,000 km^3 threshold (Figure 3) and some more its lower uncertainty bounds. On the other hand, within

the limitations of our reconstruction approach, our results clearly indicate the absence of extremely likely (99.9%) and very likely (99%) major deep water formation events during this period.

Independent of the exact timing of event years and their attribution to large volcanic eruptions or the AO/NAO state, our results indicate more frequent major Red Sea deep water formation events prior to ~1900, and in particular prior to ~1850 during the late LIA, compared to the twentieth century (Figure 3). An explanation could be the slightly cooler conditions prior to ~1900, and in particular the more arid conditions prior to ~1850, indicated for the northern Red Sea by paired Sr/Ca and $\delta^{18}O$ records of the same coral (Felis et al., 2018). This change in mean climate toward cooling and increased surface evaporation has likely provided conditions that favored deep water formation events, which ultimately resulted from the superimposed interannual atmospheric variability not exclusively related to large volcanic eruptions or the AO/NAO (Figure 4). Note that large tropical volcanic eruptions were also more frequent at that time, in particular during the first half of the nineteenth century at the end of the LIA (Figures 3 and 4 and Table 1). Importantly, our results suggest that the rapid 1982–2001 Red Sea deep water renewals indicated by hydrographic observations and ocean-atmosphere modeling (Yao & Hoteit, 2018) were the result of an unusual clustering of large tropical volcanic eruptions (El Chichón 1982 and Pinatubo 1991) and winters with strong positive AO/NAO phase (e.g., 1989) and were probably unusual in the context of the entire twentieth century.

7. Conclusions

Our study has implications for estimates of Red Sea deep water renewal time. Whereas repeated hydrographic observations and ocean-atmosphere modeling during 1982–2001 suggest a renewal time on the order of a decade as inferred from rapid renewals where large portions of the deep water were episodically renewed (Yao & Hoteit, 2018), earlier estimates inferred from a few synoptic observations since the 1960s and more simplified models suggested a sluggish renewal time of 36 to 90 years (Cember, 1988; Eshel et al., 1994; Woelk & Quadfasel, 1996). Our new coral reconstruction provides a continuous, annually resolved long-term perspective suggesting an absence of major deep water formation events during an ~100-year-long time interval (1884–1981) but indicating more frequent events prior to ~1850 during the late LIA. Thus, our results suggest that Red Sea deep water renewal time can be on the order of a decade up to a century and is dependent on the mean climatic conditions as well as on the large-scale interannual climate forcing, which both vary through time. Furthermore, the Red Sea hosts some of the most productive and diverse coral reefs, and northern Red Sea reefs are considered as refugia from global warming and ocean acidification (Fine et al., 2019). As deep vertical water mass mixing events can have severe impacts on coral reefs of the area (Felis et al., 1998; Genin et al., 1995), improved knowledge of their pacing is essential for future management strategies of these unique ecosystems. Our study emphasizes the importance of annually resolved marine proxy records in extending hydrographic observations into the preinstrumental period, in order to place recent atmosphere-ocean dynamics and surface ocean-deep ocean interactions into a long-term context.

Acknowledgments
We thank F. Yao and I. Hoteit of KAUST (Thuwal, Saudi Arabia) for making their model data available to us, M. Toohey of GEOMAR (Kiel, Germany) for providing the VSSI data, H. Kuhnert of MARUM (Bremen, Germany), and G. Lohmann of AWI (Bremerhaven, Germany) for comments on earlier versions of the manuscript. T. F. acknowledges MARUM - Center for Marine Environmental Sciences at the University of Bremen (Germany) for support. The coral data for this paper are available at the World Data Center PANGAEA (https://doi.pangaea.de/10.1594/PANGAEA.900471).

References

Cember, R. P. (1988). On the sources, formation, and circulation of Red Sea deep water. *Journal of Geophysical Research*, *93*(C7), 8175–8191. https://doi.org/10.1029/JC093iC07p08175

Craig, H. (1966). Isotopic composition and origin of the Red Sea and Salton Sea geothermal brines. *Science*, *154*(3756), 1544–1548. https://doi.org/10.1126/science.154.3756.1544

Eshel, G., Cane, M. A., & Blumenthal, M. B. (1994). Modes of subsurface, intermediate, and deep water renewal in the Red Sea. *Journal of Geophysical Research*, *99*(C8), 15,941–15,952. https://doi.org/10.1029/94JC01131

Eshel, G., & Naik, N. H. (1997). Climatological coastal jet collision, intermediate water formation, and the general circulation of the Red Sea. *Journal of Physical Oceanography*, *27*(7), 1233–1257. https://doi.org/10.1175/1520-0485(1997)027%3C1233:CCJCIW%3E2.0.CO;2

Eshel, G., Schrag, D. P., & Farrell, B. F. (2000). Troposphere-planetary boundary layer interaction and the evolution of ocean surface density: Lessons from Red Sea corals. *Journal of Climate*, *13*(2), 339–351. https://doi.org/10.1175/1520-0442(2000)013%3C0339:TPBLIA%3E2.0.CO;2

Felis, T. (2001). Stable isotope analysis on *Porites* coral core RUS-95 from the Red Sea. https://doi.org/10.1594/PANGAEA.65773

Felis, T., Ionita, M., Rimbu, N., Lohmann, G., & Kölling, M. (2018). Mild and arid climate in the eastern Sahara-Arabian Desert during the late Little Ice Age. *Geophysical Research Letters*, *45*(14), 7112–7119. https://doi.org/10.1029/2018GL078617

Felis, T., Pätzold, J., Loya, Y., Fine, M., Nawar, A. H., & Wefer, G. (2000). A coral oxygen isotope record from the northern Red Sea documenting NAO, ENSO, and North Pacific teleconnections on Middle East climate variability since the year 1750. *Paleoceanography*, *15*(6), 679–694. https://doi.org/10.1029/1999PA000477

Felis, T., Pätzold, J., Loya, Y., & Wefer, G. (1998). Vertical water mass mixing and plankton blooms recorded in skeletal stable carbon isotopes of a Red Sea coral. *Journal of Geophysical Research*, *103*(C13), 30,731–30,739. https://doi.org/10.1029/98JC02711

Fine, M., Cinar, M., Voolstra, C. R., Safa, A., Rinkevich, B., Laffoley, D., et al. (2019). Coral reefs of the Red Sea—Challenges and potential solutions. *Regional Studies in Marine Science*, *25*, 100498. https://doi.org/10.1016/j.rsma.2018.100498

Gao, C., Robock, A., & Ammann, C. (2008). Volcanic forcing of climate over the past 1500 years: An improved ice core-based index for climate models. *Journal of Geophysical Research*, *113*, D23111. https://doi.org/10.1029/2008JD010239

Genin, A., Lazar, B., & Brenner, S. (1995). Vertical mixing and coral death in the Red Sea following the eruption of Mount Pinatubo. *Nature*, *377*(6549), 507–510. https://doi.org/10.1038/377507a0

Global Volcanism Program (2013). In E. Venzke (Ed.), *Volcanoes of the world* (Vol. 4.7.5). Washington, DC: Smithsonian Institution. Downloaded 11 Dec 2018. https://doi.org/10.5479/si.GVP.VOTW4-2013

Jones, P. D., Jonsson, T., & Wheeler, D. (1997). Extension to the North Atlantic Oscillation using early instrumental pressure observations from Gibraltar and south-west Iceland. *International Journal of Climatology*, *17*(13), 1433–1450. https://doi.org/10.1002/(SICI)1097-0088(19971115)17:13%3C1433::AID-JOC203%3E3.0.CO;2-P

Luterbacher, J., & Pfister, C. (2015). The year without a summer. *Nature Geoscience*, *8*(4), 246–248. https://doi.org/10.1038/ngeo2404

Mudelsee, M. (2014). *Climate time series analysis: Classical statistical and bootstrap methods* (2nd ed.). Cham, Switzerland: Springer. https://doi.org/10.1007/978-3-319-04450-7

Osborn, T. J. (2011). Winter 2009/2010 temperatures and a record-breaking North Atlantic Oscillation index. *Weather*, *66*(1), 19–21. https://doi.org/10.1002/wea.660

Rimbu, N., Lohmann, G., Felis, T., & Pätzold, J. (2001). Arctic Oscillation signature in a Red Sea coral. *Geophysical Research Letters*, *28*(15), 2959–2962. https://doi.org/10.1029/2001GL013083

Robock, A. (2015). Climatic impacts of volcanic eruptions. In H. Sigurdsson (Ed.), *The encyclopedia of volcanoes* (2nd ed., pp. 935–942). Amsterdam: Academic Press. https://doi.org/10.1016/B978-0-12-385938-9.00053-5

Robock, A., & Mao, J. (1992). Winter warming from large volcanic eruptions. *Geophysical Research Letters*, *19*(24), 2405–2408. https://doi.org/10.1029/92GL02627

Rohling, E. J., Grant, K., Bolshaw, M., Roberts, A. P., Siddall, M., Hemleben, C., & Kucera, M. (2009). Antarctic temperature and global sea level closely coupled over the past five glacial cycles. *Nature Geoscience*, *2*(7), 500–504. https://doi.org/10.1038/ngeo557

Schlitzer, R. (2018). Ocean data view. Retrieved from https://odv.awi.de/

Toohey, M., Krüger, K., Schmidt, H., Timmreck, C., Sigl, M., Stoffel, M., & Wilson, R. (2019). Disproportionately strong climate forcing from extratropical explosive volcanic eruptions. *Nature Geoscience*, *12*(2), 100–107. https://doi.org/10.1038/s41561-018-0286-2

Toohey, M., & Sigl, M. (2017). Volcanic stratospheric sulfur injections and aerosol optical depth from 500 BCE to 1900 CE. *Earth System Science Data*, *9*(2), 809–831. https://doi.org/10.5194/essd-9-809-2017

Woelk, S., & Quadfasel, D. (1996). Renewal of deep water in the Red Sea during 1982–1987. *Journal of Geophysical Research*, *101*(C8), 18,155–18,165. https://doi.org/10.1029/96JC01148

Yao, F., & Hoteit, I. (2018). Rapid Red Sea deep water renewals caused by volcanic eruptions and the North Atlantic Oscillation. *Science Advances*, *4*(6), eaar5637. https://doi.org/10.1126/sciadv.aar5637

Zambri, B., & Robock, A. (2016). Winter warming and summer monsoon reduction after volcanic eruptions in Coupled Model Intercomparison Project 5 (CMIP5) simulations. *Geophysical Research Letters*, *43*, 10,920–10,928. https://doi.org/10.1002/2016GL070460

Geophysical Research Letters

Supporting Information for

Pacing of Red Sea deep water renewal during the last centuries

Thomas Felis[1] and Manfred Mudelsee[2,3]

[1]MARUM – Center for Marine Environmental Sciences, University of Bremen, Bremen, Germany.

[2]Climate Risk Analysis, Heckenbeck, Bad Gandersheim, Germany.

[3]Alfred Wegener Institute Helmholtz Centre for Polar and Marine Research, Bremerhaven, Germany.

Contents of this file

Introduction

The supporting information gives more details on material and methods, including the coral record and chronology, the coral proxy calibration, the statistical information, and the model simulation.

Text S1.

Material and Methods

Coral record and chronology

An annually resolved proxy time series of winter conditions in northern Red Sea surface waters was obtained from a $\delta^{18}O$ record (Felis et al., 2000) of a shallow-water coral growing at Ras Umm Sidd (34°18.6'E, 27°50.9'N) near the southern tip of the Sinai Peninsula (Egypt), a site directly exposed to open northern Red Sea waters (Felis et al., 2000) (Fig. 1). The time series was derived from the annual winter maxima of subseasonally analysed $\delta^{18}O$ values in the aragonitic skeleton of a massive *Porites* colony (Felis, 2001; Felis et al., 2000) (core/colony RUS-95) due to the better detectability of extreme events, instead of the interpolated bimonthly resolution $\delta^{18}O$ record interpreted in previous studies (Felis et al., 2018; Felis et al., 2000; Rimbu et al., 2001). The chronology construction was previously described (Felis et al., 2000). The $\delta^{18}O$ record shows clear annual cycles, which can be counted back to the year 1750. This age model is corroborated by the skeletal pattern of annual density-band pairs. Therefore, the annual chronology obtained by counting from the living coral surface to the bottom of the core can be assumed to be without age model error in the interval 1995-1925. Due to minor uncertainties associated with a change in the microsampling transect at the transition between slabbed core segments in two cases, an age model error of ±1 year was assigned to the interval 1924-1783 and ±2 years to the interval 1782-1750.

Coral proxy calibration

The winter coral $\delta^{18}O$ time series was calibrated with modelled changes in the total volume of the annual contributions from open-ocean deep convection and combined outflows from the Gulfs of Suez and Aqaba to wintertime deep water formation in the northern Red Sea, as derived from simulations of an ocean general circulation model with realistic atmospheric forcing (Yao & Hoteit, 2018). The period of overlap between the coral record and the model simulation (1982-1995) encompasses three major (1983, 1992, and 1993), one minor (1989), and one very minor (1990) deep water formation event, as well as nine years without significant deep water formation (Yao & Hoteit, 2018). An ordinary least squares regression with bias correction (Mudelsee, 2014) (OLSBC) was applied to the data (five event years plus the weighted average of the nine non-event years), which reveals a significant relationship between total volume of deep water formation and winter coral $\delta^{18}O$ (~52000 ± 32000 km^3 per ‰) (Fig. 2). Based on the OLSBC regression, we define a major deep water formation event as having a total volume of >20,000 km^3 or coral $\delta^{18}O$ of >–2.78‰.

Statistical information

For the quantification of the relationship between total volume of deep water formation and winter coral $\delta^{18}O$ on the $n = 6$ data pairs (Fig. 2), we employed OLSBC regression (Mudelsee, 2014). The OLSBC correction factor is given by $(1 - f)^{-1}$, where f is the ratio of the $\delta^{18}O$ measurement error (0.07‰) squared and the variance of the $\delta^{18}O$ values (0.0352‰²). The slope, estimated using ordinary least squares, is multiplied by the correction factor (1.16) in order to correct for a negative bias caused by the presence of predictor ($\delta^{18}O$) uncertainties. The standard error of the OLSBC slope estimate was determined by means of bootstrap resampling (Mudelsee, 2014), for which autocorrelation effects were negligible. The significance of the OLSBC slope estimate (52223 ± 31738 km^3 per ‰) was confirmed using Pearson's correlation coefficient with 95% bootstrap confidence interval ($r = 0.69$ [0.47; 0.83])

(Mudelsee, 2014). For the determination of the upper uncertainty bounds for the coral $\delta^{18}O$ threshold (Fig. 3), we employed Gaussian error propagation (Mudelsee, 2014), that is, the one-sided 99.9%-level corresponds to 3.09-sigma and the 99%-level to 2.33-sigma. The lower uncertainty bounds are obtained in a similar way. We note that considering a detrended winter coral $\delta^{18}O$ time series for establishing the calibration with total volume of deep water formation may principally improve the fit. However, we prefer not to pursue this approach further since the number of data pairs (n = 6) is rather small and a simple statistical method, which avoids overfitting, is therefore applied.

Model simulation

The model simulation (Yao & Hoteit, 2018) used to calibrate the winter coral $\delta^{18}O$ time series is a high-resolution Massachusetts Institute of Technology general circulation model (Marshall et al., 1997) (MITgcm) simulation for the period 1979-2001 (40 vertical levels, horizontal resolution of ~1.5 km, including the Gulf of Aqaba, the Gulf of Suez, the Red Sea, and the western part of the Gulf of Aden), forced by atmospheric reanalysis data (Dee et al., 2011) (ERA-Interim) produced by the European Centre for Medium-Range Weather Forecasts. For calibration, we used the modelled changes in the total volume of the annual contributions to wintertime deep water formation in the northern Red Sea, calculated by summing up the modelled annual contributions from open-ocean deep convection and combined outflows from the Gulfs of Suez and Aqaba (Yao & Hoteit, 2018).

References

Dee, D. P., Uppala, S. M., Simmons, A. J., Berrisford, P., Poli, P., Kobayashi, S., et al. (2011). The ERA-Interim reanalysis: configuration and performance of the data assimilation system. *Quarterly Journal of the Royal Meteorological Society*, *137*, 553-597. https://rmets.onlinelibrary.wiley.com/doi/abs/10.1002/qj.828

Felis, T. (2001). Stable isotope analysis on *Porites* coral core RUS-95 from the Red Sea. https://doi.org/10.1594/PANGAEA.65773

Felis, T., Ionita, M., Rimbu, N., Lohmann, G., & Kölling, M. (2018). Mild and arid climate in the eastern Sahara-Arabian Desert during the late Little Ice Age. *Geophysical Research Letters*, *45*, 7112-7119. https://doi.org/10.1029/2018GL078617

Felis, T., Pätzold, J., Loya, Y., Fine, M., Nawar, A. H., & Wefer, G. (2000). A coral oxygen isotope record from the northern Red Sea documenting NAO, ENSO, and North Pacific teleconnections on Middle East climate variability since the year 1750. *Paleoceanography*, *15*, 679-694. https://doi.org/10.1029/1999PA000477

Marshall, J., Hill, C., Perelman, L., & Adcroft, A. (1997). Hydrostatic, quasi-hydrostatic, and nonhydrostatic ocean modeling. *Journal of Geophysical Research: Oceans*, *102*, 5733-5752. https://doi.org/10.1029/96JC02776

Mudelsee, M. (2014). *Climate Time Series Analysis: Classical Statistical and Bootstrap Methods* (2nd ed.). Cham, Switzerland: Springer. https://doi.org/10.1007/978-3-319-04450-7

Osborn, T. J. (2011). Winter 2009/2010 temperatures and a record-breaking North Atlantic Oscillation index. *Weather*, *66*, 19-21. https://doi.org/10.1002/wea.660

Rimbu, N., Lohmann, G., Felis, T., & Pätzold, J. (2001). Arctic Oscillation signature in a Red Sea coral. *Geophysical Research Letters*, *28*, 2959-2962. https://doi.org/10.1029/2001GL013083

Yao, F., & Hoteit, I. (2018). Rapid Red Sea Deep Water renewals caused by volcanic eruptions and the North Atlantic Oscillation. *Science Advances*, *4*, eaar5637. https://doi.org/10.1126/sciadv.aar5637